RESEARCH ARTICLE

Elastic Surface Model For Beta-Barrels: Geometric, Computational, And Statistical Analysis

Magdalena Toda | Fangyuan Zhang | Bhagya Athukorallage [iD]

Department of Mathematics and Statistics, Texas Tech University, Lubbock, Texas 79409

Correspondence
Bhagya Athukorallage, Department of Mathematics and Statistics, Texas Tech University, Lubbock, TX 79409.
Email: bhagya.athukorala@ttu.edu

Abstract

Over the past 2 decades, many different geometric models were created for beta barrels, including, but not limited to: cylinders, 1-sheeted hyperboloids, twisted hyperboloids, catenoids, and so forth. We are proponents of an elastic surface model for beta-barrels, which includes the minimal surface model as a particular case, but is a lot more comprehensive. Beta barrel models are obtained as numerical solutions of a boundary value problem, using the COMSOL Multiphysics Modeling Software. We have compared them against the best fitting statistical models, with positive results. The geometry of each individual beta barrel, as a rotational elastic surface, is determined by the ratio between the exterior diameter and the height. Through our COMSOL computational modeling, we created a rather large variety of generalized Willmore surfaces that may represent models for beta barrels. The catenoid is just a particular solution among all these shapes.

KEYWORDS
beta barrel, generalized Willmore energy, mean curvature, minimal surface, protein structure

1 | INTRODUCTION

In biochemistry, biophysics and mathematical biology, secondary structures represent the main types of local surfaces (shapes) corresponding to biopolymers (eg, proteins and nucleic acids). On a finer level, the atomic positions in 3D space are said to form the tertiary structure.

The most common secondary structures are the alpha helices. The second most-common are the beta sheets and beta barrels. A beta barrel is a collection of beta-sheets that twist and coil in a shape that can be described as a smooth surface of revolution which resembles a barrel. In this structure, the first strand is hydrogen bonded to the last. Beta-strands in beta-barrels are typically arranged in an antiparallel fashion. Barrel structures are commonly found in proteins that span cell membranes and in proteins that bind hydrophobic ligands in the barrel center.

A beta barrel represents an ideal smooth surface described by the beta strands. The most common type, the so called up-and-down barrel, is considered to be a surface of revolution that is topologically equivalent to a cylinder. Up-and-down barrels consist of a series of beta strands, each of which is hydrogen-bonded to the strands immediately before and after it in the primary sequence. Beta-strands in beta-barrels are typically arranged in an antiparallel fashion, but some proteins, such as the green fluorescent protein (GFP), are characterized by beta barrels formed with both parallel and antiparallel beta strands. Beta barrel structures (named for their resemblance to the barrels that hold liquids) are commonly found in porins and other proteins that span cell membranes, and in proteins that bind hydrophobic ligands in the barrel center, as in lipocalins.

In many cases, the strands contain alternating polar and hydrophobic amino acids, so that the hydrophobic residues are oriented toward the interior of the barrel to form a hydrophobic core and the polar residues are oriented toward the outside of the barrel on the solvent-exposed surface. Porins and other membrane proteins containing beta barrels reverse this pattern, with hydrophobic residues oriented toward the exterior where they contact the surrounding lipids, and hydrophilic residues oriented toward the interior pore.

The polyhedral, discrete skeleton of beta-barrels can be classified in terms of 2 integer parameters: the number of strands in the beta-sheet, n, and the "shear number", S, a measure of the stagger of the strands in the beta-sheet. These 2 parameters (n and S) are related to the inclination angle of the beta strands relative to the axis of the barrel. To us, the number of strands and the sheer number are irrelevant. We consider the best fitting smooth surface for this polyhedral molecular skeleton, to be what we refer to as beta barrel.

Several models were proposed for beta sheets and beta barrels. Among them, we recall, in chronological order: the twisted 1-sheeted

TABLE 1 Mean curvature values of beta barrels for several types of proteins (from reference[4])

Protein	Average of mean curvature	SD of mean curvature
Triose phosphate isomerase	0.040	0.021
Taka-amylase	0.035	0.007
Glycolate-oxidase	0.035	0.007
Trimethanolamine dehydrogenase	0.037	0.013
Cytochrome b2	0.033	0.005
Aldolase	0.035	0.112

hyperboloid (see,[1] 1984), followed by the usual 1-sheeted hyperboloid (see,[2] 1988), and much later, the catenoid as a best-fit (see,[3] 2005). Over time, all the above-mentioned surfaces have been tried as "best models" for beta barrels. We became aware of the fact that none of these models is satisfactory. A few authors presented arguments based on experimental data that the beta sheet structures in proteins are the result of the tendency to minimize surface areas, and should therefore be very close to minimal surfaces. For a large diversity of aminoacids, the mean curvature was experimentally measured and it turned out to be close to a specific constant, which is small in absolute value, but not negligible. A decade ago, Koh and Kim[3] have proposed the model that all beta-sheet structures "are almost minimal surfaces". By this, they meant that their mean curvatures are very small, but the term almost-minimal has no mathematical foundation.

We would like to make it clear, however, that while the mean curvature could be small in absolute value for some beta barrels, it may be far away from zero for others, and it may also vary significantly from a point to another of the same barrel. Koh and Kim stated: "The fact that the commonly used models for some beta-sheet surfaces (ie, the hyperboloid and strophoid) have very small mean curvatures (under 0.05) supports our model". For example, for the following enzymes: glycolate-oxidase, taka-amylase, and aldolase, the mean curvature H, measured experimentally for beta-sheets, is approximately $H = 0.039$ (for each of them). In reference,[4] the authors presented the mean curvature values for several aminoacids, and are depicted in Table 1. On the other hand, the mean curvature values may change significantly from a type of protein to another.

Moving in a new direction, that can give us a better view, we are proponents of an "elastic surface model for beta-barrels", which includes the minimal surface model as a particular case, but is a lot more comprehensive. Such a model has already been proposed in part by[5] for beta sheets with antiparallel strands. We study beta barrels as elastic surfaces, and obtain them as numerical solutions of a boundary value problem—while comparing them against the best fitting statistical models. It is important to remark that catenoids represent the only minimal surfaces of revolution, and in particular, they are Willmore-type surfaces (elastic surfaces) [14]. As such, they are included in our model. Through our COMSOL computational modeling, we created a rather large variety of Willmore-type surfaces that may represent models for beta barrels.

As a relevant real-world application of high relevance and actuality, observe the model of the beta barrel of GFP in Figure 1 and remark its unduloidal shape (Delaunay-type unduloid). Martin Chalfie, Osamu Shimomura, and Roger Y. Tsien were awarded the 2008 Nobel Prize in Chemistry for their discovery and development of the GFP model. On the other hand, Helfrich [10] has introduced the curvature energy per unit area, corresponding to bio-membranes (lipid bilayers) as:

$$E_{lb} = \int_M k_c(2H+c_0)^2 + \bar{k}K \, dS, \tag{1}$$

where k_c and $\bar{k}$ represent specific rigidity constants, H and K are the mean and Gaussian curvatures of the surface M, respectively, while c_0 is the so-called spontaneous curvature.

We would like to mention that this type of generalized bending energy (at times referred to as Helfrich-type energy) has been considered for other types of elastic membranes in biophysics, as well, e.g. [6], [7], [11], [12]. Following the model proposed by Helfrich, two other scientists, S. Choe and X.S. Sun, proposed a similar elastic model for anti-parallel beta sheets, which was published in 2007 in the Biophysical Journal[5]—based on a bending energy, namely:

$$E_{lb} = \int_M [k(H+c_0)^2 + \bar{k}K] \, dS, \tag{2}$$

where dS is the infinitesimal area, c_0 is the "preferred curvature of the surface" as they call it, and k and $\tilde{k}$ are bending moduli that "relate the energy change with changes in mean and Gaussian curvatures".

Our elastic surface model for beta barrels is similar to this model, with the exception of an added constant term that comes from the superficial tension combined with a stress tensor, and with the additional assumption that c_0 is negligible. We therefore write

$$E_b = \int_M [kH^2 + \tilde{k}K + \mu] \, dS, \tag{3}$$
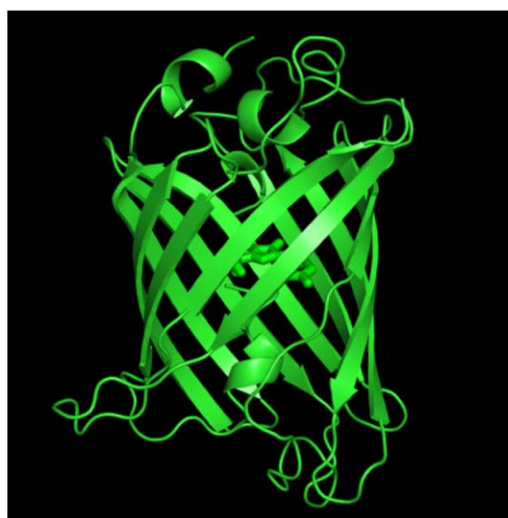
FIGURE 1 Beta Barrel of the GFP (from jelly fish) by scientists Martin Chalfie, Osamu Shimomura and Roger Tsien—Nobel prize recipients (courtesy of the American Association of Clinical Chemistry) [Color figure can be viewed at wileyonlinelibrary.com]
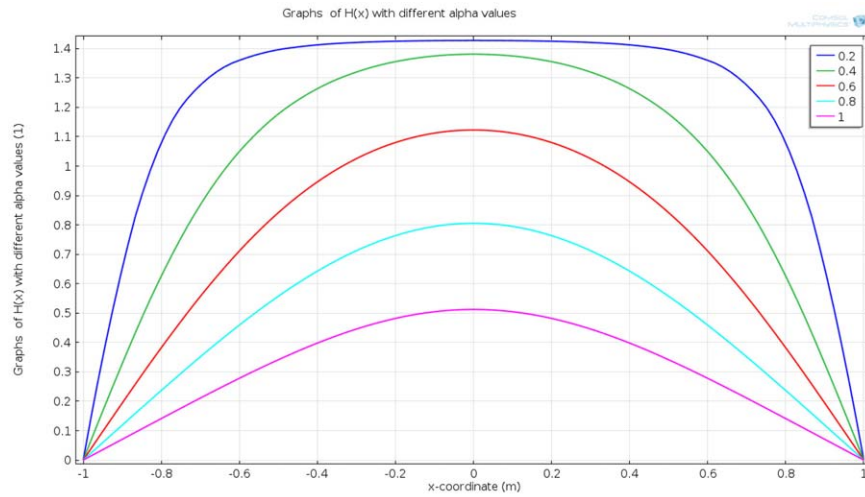
(A) $H(x)$ *with* $\epsilon = 0.1$
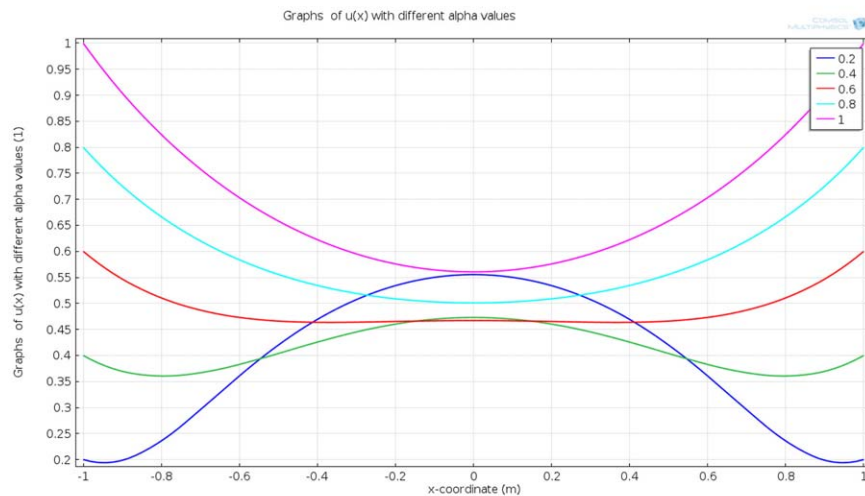
(B) $u(x)$ *with* $\epsilon = 0.1$

FIGURE 2 Solutions to our boundary value problem, as $H(x)$, and corresponding profile curves $u(x)$ for different α values and for fixed ϵ value [Color figure can be viewed at wileyonlinelibrary.com]

and call this type of energy generalized Willmore energy (GW energy), or generalized bending energy. The Euler-Lagrange equation corresponding to the GW energy functional can be written as the following (GWE):

$$\Delta_g(H) + 2H(H^2 - K - \epsilon) = 0, \tag{4}$$

where $\epsilon = \mu/k$ and Δ_g represents the Laplace-Beltrami operator corresponding to the metric g that is naturally induced by the surface parameterization. We are interested in rotational surfaces that represent minimizers of GW energy (that is, solutions to its corresponding Euler-Lagrange equation described above). These represent our general models for beta barrels. Hereby, we are recalling the basics of a computational study that we have performed on this type of surfaces, in.[7] Consider a Cartesian system of axes of coordinates x, y, z in $\mathbb{R}^3$ and the circles C_1, C_2 of the same radius α, centered at $(-1, 0, 0)$ and $(1, 0, 0)$, situated in planes orthogonal to the x axis. Consider all regular surfaces of revolution of annular-type with boundary $C_1 \cup C_2$. Assume that

among all these surfaces, there exists at least a surface M minimizing the GWE. This surface in assumed embedded in $\mathbb{R}^3$ and admitting the representation

$$M := \{x, u(x)\cos\varphi, u(x)\sin\varphi\} : x \in [-1, 1], \varphi \in [0, 2\pi],$$

where $u \in C^4([-1, 1], (0, \infty))$ represents the profile function. Then, the surface M is a solution of the following boundary value problem:

$$\Delta H + 2H(H^2 - K - \epsilon) = 0 \quad \text{on } M, \text{ where } \epsilon = \frac{\mu}{k} \tag{5}$$

$$H = 0 \quad \text{on } \partial M = C_1 \cup C_2, \tag{6}$$

$$u(\pm 1) = \alpha. \tag{7}$$

In these assumptions, there exists a positive value α^* ($\alpha^* \approx 1.5089$) that is independent from the value of ϵ, such that

a If $0 < \alpha < \alpha^*$, then GWE admits NO minimal solution, that is, any solution satisfies: $H = 0$ on ∂M and $H \neq 0$ on $M \setminus (\partial M)$.
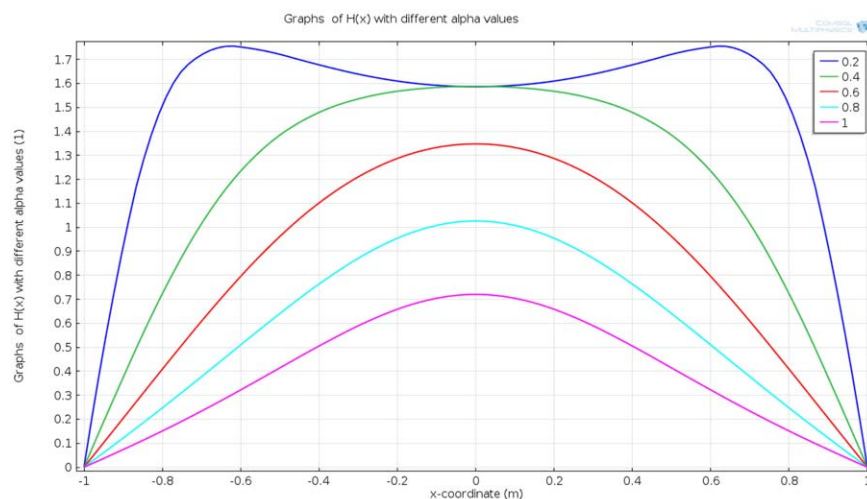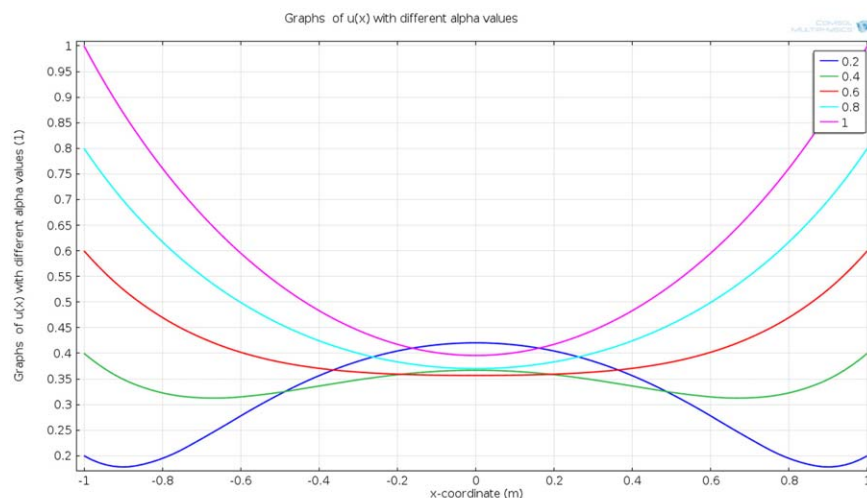
(A) $H(x)$ with $\epsilon = 1$

(B) $u(x)$ with $\epsilon = 1$

FIGURE 3 Solutions to our boundary value problem, as *H(x)*, and corresponding profile curves *u(x)* for different α values and for fixed ϵ value [Color figure can be viewed at wileyonlinelibrary.com]

b If $\alpha = \alpha^*$, then GWE admits exactly 1 minimal solution (a unique catenoid that exclusively depends on α^*).

c If $\alpha > \alpha^*$, then GWE admits exactly 2 minimal solutions (2 catenoids whose equations exclusively depend on α).

The proof is straight-forward, as based on elementary arguments, and can be found in.[7] Such a Dirichlet boundary value problem was posed for the Willmore equation in [9].

Further, we have analyzed the α-family of solutions that corresponds to various fixed values of ϵ. We were able to construct corresponding families of solutions using COMSOL Multiplysics, see fig. 2 and 3. On the other hand, of course, each solution to our boundary value problem (and in particular each catenoidal solution) can actually be represented in COMSOL, if we choose the unique value α appropriately, and deal with the solution branching (in order to graph all corresponding solutions *u* if that is the case).

Remark the shapes obtained for the profile *u(x)* as solutions to the boundary value problem associated to GWE, in all the figures presented in this article: they resemble either a catenary, or an undulary—thus generating catenoidal and unduloidal GW surfaces of revolution. Due to the physical nature of our boundary value problem, the nodoidal solutions are absent, but nodoidal solutions would certainly be present for other types of boundary value conditions of the GWE. Following our analysis, for each and every value of α that is higher than α^*, there exist 3 distinct solutions, namely 2 catenoidal profiles and a non-minimal solution—which could be unstable (that is, not a local minimizer of the energy). Remark that catenoids represent global minimizers, as Deckelnick and Grunau[8] showed in a recent article. For the classical Willmore case $\epsilon = 0$, authors proved that the non-minimal solution is contained between the 2 catenoids, and it is unstable. Our numerical analysis on the stability of the solutions to the GWE is in progress (Figures 2 and 3).

Beta barrels are hereby represented as solutions of the boundary value problem of the GW equation, GWE. Let *D* represent the "exterior diameter" of the beta barrel, which is defined as the diameter of the end-circles (what we call the imaginary top and bottom of the beta barrel). Let *h* represent the distance between these two circles, which is informally referred as the *height* of the beta barrel. Considering the mathematical model of the beta barrel (solution of our boundary value problems), its corresponding height will be 2 (distance between −1 and 1 on the *x* axis). Correspondingly, the diameter of the "bottom and top circles" will be 2α. Therefore, the meaning of the α parameter from the mathematical model is that of the ratio between diameter and height, namely D/h, of the real-life beta barrel.

Elasticity theory provides enough reasons for the validity of our computational PDE model. On the other hand, we decided to strengthen our arguments by making an unbiased comparison between our computational model (solution of the boundary value problem) and the statistical models that correspond to protein databases.

2 | MATERIALS AND METHODS

2.1 | Beta barrel structure dataset from GFP class

To test the performance of the elastic surface model, we used the GFP C_α coordinates dataset from Protein Data Bank. Out of the 54 proteins, we excluded 10 with more than 1 domain, and extracted the structure information using Dictionary of Protein Secondary Structure files. We considered only "E" segments that form intradomain β-ladders as β-strands.

2.2 | Least square estimation using 3 models

We used least square estimation (LSE) to compare the elastic surface model with 2 other models: catenoid and cylinder. In Cartesian system, the coordinates of a catenoid (*x*, *y*, *z*) need to satisfy the following equations:

$$\begin{cases} r = a \cosh\left(\dfrac{z}{a}\right) \\ x = r \cos\left(2\pi f\right) \\ y = r \sin\left(2\pi f\right) \end{cases}$$

We used 211 equally spaced *a* values from 0.4 to 2.5. For each *a* value, we generated 300 equally spaced points from −1 to +1 for the variable *z*, and 100 points from 0 to 1 for *f*. Therefore, we obtained 30,000 points for each catenoid with a different *a* value. The diameter/height ratio $a \cosh\left(\frac{1}{a}\right)$ ranges from 1.5 to 2.7. In Cartesian system, the coordinates of a cylinder (*x*, *y*, *z*) need to satisfy the following equations:

$$\begin{cases} r \text{ is a constant for given } z \\ x = r \cos\left(2f\pi\right) \\ y = r \sin\left(2f\pi\right) \end{cases}$$

For the variable *r*, we used 100 equally spaced points, namely from from 0.7 to 1.7. For each *r* value, we generated 300 equally

spaced points from −1 to +1 for *z* and, respectively, 100 points from 0 to 1 for *f*. Therefore, we get 30, 000 points for each cylinder with a different *r* value. The diameter/height ratio *r* ranges from 0.7 to 1.7. For the elastic surface model, we used 89 equally spaced ϵ values from 0 to 0.88, and 48 equally spaced diameter/height values α from 0.7 to 1.17. For each of ϵ and α combinations, we generated 300 equally spaced points from −1 to +1 for *z*, and 100 points from 0 to 1 for *f*, respectively. Therefore, by using COMSOL Multiplysics, we obtained 30,000 points for each elastic surface, with different ϵ and α values.

The procedure to get the LSE for the 3 models can be described as follows:

1. *S* denotes one simulated dataset. *D* denotes the C_α coordinates data for a certain protein. Denote *n* as the number of points in dataset *D*.

2. Randomly select *n* points from *S*, denoted as *s*. Denote $d = D$.

3. Run Procrustes analysis for optimal modeling, up to translating, rotating, and scaling *d* to superimpose to *s*. *d* is updated as the transformed data. The scale value is recorded.

4. Search in dataset *S* to find *n* points closest to each of the points in *d*, denoted as *s*.

5. Repeat steps steps 3) and 4) 10,000 times, and record *d* with the least sum of squares for error (SSE) from the subset *s* in the iteration, denoted as d_0 and s_0 with series of scale values as $c_1, c_2, \ldots, c_t$.

6. Denote $d_1 = d_0/(c_1 c_2 \cdots c_t)$ as the transformed real data in the original scale. Apply the same translating, rotating, and scaling procedure on *S* as the one to optimally superimpose s_0 to d_1. The result is denoted as S_1.

7. Apply the Iterative Closest Point method to match S_1 to d_1, resulting in rotated data S_2. Then get correspondences in S_2 using nearest neighbor search, denoted as s_2.

8. Calculate SSE between s_2 and d_1.

For each model, we run the above procedure to find the best parameter value to achieve the smallest SSE. The results are shown in the following table.

3 | RESULTS AND DISCUSSION

3.1 | Statistical model comparison with the computational models in COMSOL

We can see from Table 2 that almost all of the roots of mean squares for error (RMSE) are smaller than 3, by fitting the 3 models, except proteins 1f09 and 1qyf. It turns out that the 3D structures of these 2 proteins are quite different from the others. Further investigation is needed in order to fit the two proteins using other more proper models. For all the other proteins, the elastic surface model achieves its smallest RMSE when the estimated diameter/height ratio ranges between 0.83 and 0.89. The cylindrical beta barrel model corresponds

TABLE 2 LSE results for GFP by using 3 models

	Catenoid			Cylinder		Elastic surface		
	a	diam./ht.	RMSE	diam./ht.	RMSE	epsilon	diam./ht.	RMSE
1bfp	0.76	1.518	2.582	0.73	1.371	0.67	0.85	1.318
1c4f	0.8	1.511	2.569	0.74	1.354	0.68	0.86	1.306
1cv7	0.81	1.510	2.496	0.77	1.373	0.69	0.88	1.323
1ema	0.77	1.516	2.539	0.71	1.356	0.64	0.85	1.296
1emb	0.76	1.518	2.578	0.73	1.375	0.67	0.86	1.318
1emf	0.79	1.512	2.527	0.72	1.359	0.63	0.85	1.293
1emg	0.79	1.512	2.549	0.72	1.351	0.66	0.85	1.300
1emk	0.76	1.518	2.549	0.7	1.339	0.64	0.84	1.295
1eml	0.8	1.511	2.560	0.72	1.373	0.62	0.85	1.327
1emm	0.76	1.518	2.540	0.72	1.380	0.66	0.87	1.322
1f0b	0.76	1.518	2.575	0.72	1.369	0.71	0.88	1.316
1f09	0.4	2.453	5.128	0.56	4.564	0.02	0.7	4.566
1huy	0.75	1.521	2.556	0.74	1.411	0.63	0.88	1.345
1jby	0.77	1.516	2.590	0.74	1.361	0.67	0.87	1.321
1jbz	0.78	1.514	2.506	0.74	1.362	0.63	0.89	1.277
1kyp	0.77	1.516	2.566	0.71	1.404	0.66	0.87	1.348
1kyr	0.76	1.518	2.558	0.71	1.394	0.65	0.86	1.334
1kys	0.8	1.511	2.560	0.76	1.376	0.7	0.85	1.323
1mem	0.75	1.521	2.532	0.75	1.361	0.65	0.86	1.292
1myw	0.69	1.551	2.582	0.72	1.402	0.64	0.86	1.349
1oxd	0.74	1.525	2.598	0.72	1.387	0.68	0.86	1.337
1oxe	0.74	1.525	2.565	0.71	1.377	0.7	0.87	1.326
1oxf	0.75	1.521	2.587	0.74	1.401	0.7	0.86	1.350
1q4a	0.78	1.514	2.546	0.74	1.370	0.66	0.87	1.316
1q4b	0.75	1.521	2.571	0.72	1.372	0.64	0.88	1.322
1q4c	0.75	1.521	2.553	0.73	1.377	0.66	0.88	1.322
1q4d	0.78	1.514	2.568	0.72	1.371	0.63	0.85	1.321
1q4e	0.76	1.518	2.549	0.74	1.380	0.66	0.86	1.332
1q73	0.72	1.534	2.554	0.73	1.371	0.65	0.86	1.324
1qxt	0.78	1.514	2.524	0.74	1.344	0.67	0.86	1.281
1qy3	0.73	1.529	2.569	0.74	1.369	0.68	0.86	1.309
1qyf	0.4	2.453	5.108	0.51	4.022	0	0.7	4.124
1qyo	0.79	1.512	2.554	0.76	1.419	0.68	0.86	1.350
1qyq	0.78	1.514	2.526	0.7	1.412	0.66	0.87	1.342
1rm9	0.78	1.514	2.513	0.74	1.406	0.63	0.88	1.323
1rmm	0.77	1.516	2.536	0.72	1.387	0.67	0.87	1.318
1rmo	0.74	1.525	2.543	0.73	1.388	0.65	0.86	1.326
1rmp	0.74	1.525	2.538	0.74	1.372	0.63	0.88	1.298

(Continues)

TABLE 2 (Continued)

	Catenoid			Cylinder		Elastic surface		
	a	diam./ht.	RMSE	diam./ht.	RMSE	epsilon	diam./ht.	RMSE
1rrx	0.76	1.518	2.573	0.72	1.385	0.66	0.86	1.334
1s6z	0.79	1.512	2.598	0.71	1.418	0.67	0.86	1.365
2emd	0.76	1.518	2.537	0.74	1.402	0.6	0.87	1.321
2emn	0.71	1.539	2.695	0.72	1.435	0.59	0.86	1.356
2emo	0.78	1.514	2.498	0.71	1.335	0.65	0.84	1.290
2yfp	0.74	1.525	2.544	0.75	1.380	0.67	0.83	1.320

to a slightly higher RMSE, and similar diameter/height ratios. The catenoidal beta barrel model corresponds to a much higher RMSE and very different estimates of diameter/height ratios.

The "practical reason" for the much better fit of the elastic unduloidal-type model (when compared with its catenoidal counterpart) is the following: On one hand the GFP structure has a small diameter/height ratio, and on the other hand, while both cylinder model and elastic model can fit structures with various diameter/height ratios, the catenoidal model can only allow that ratio to be greater than (or equal to) the value $\alpha^* = 1.5089$.

The cylindrical model is close enough to the unduloidal-type elastic surface, and definitely more appropriate/accurate than the catenoid. We should not forget that, for the case when c_0 is not negligible, the GWE equation has $H = c_0$ as a stable solution. Therefore, the constant mean curvature (CMC non-zero) model may include circular cylinders, as well as true CMC unduloids. Our elastic model, together with the

statistical analysis, now make it completely clear why the GFP protein model obtained in 2008 by Chalfie, Shimomura and Tsien possesses neither a catenoidal shape, nor a round cylindrical one, but an unduloidal one (see Figure 4). The shape of the profile function u of the beta barrel is always determined by the ratio between the end-circle diameter and height (which is α). To complete the discussion, we also studied and modeled a protein example 1cka with larger diameter/height ratio. The results in Table 3 show that because the diameter/height ratio is larger for protein 1cka, catenoid model can fit better than cylinder and elastic surface model.

4 | CONCLUSION

Our elastic surface model for beta barrels proves itself to be more appropriate than the individual models that were historically used. Physical arguments led us to beta barrel models as solutions to a boundary value problem associated to a general Willmore equation. In addition, our elastic surface model satisfies the requirements of the statistical analysis, as a much better fit than previous models. This is a fortunate case, in which numerical solutions obtained via COMSOL Multiphysics (based on finite element methods) have been tested via statistical analysis, and the results were highly in favor of the elastic model.

ORCID

Bhagya Athukorallage http://orcid.org/0000-0002-1240-223X

REFERENCES

[1] Novotný J, Bruccoleri R, Newell J. Twisted hyperboloid (strophoid) as a model of beta-barrels in proteins. *J. Mol. Biol.* 1984;177(3): 567–573.

[2] Lasters I, Wodak S, Alard P, Cutsem E. Structural principles of parallel beta-barrels in proteins. *Proc Natl Acad Sci.* 1988;85(10):3338–3342.

[3] Koh E, Kim T, Cho HS. Mean curvature as a major determinant of β-sheet propensity. *Bioinformatics.* 2006;22(3):297–302.

[4] Koh E, Kim T. Minimal Surface as a Model of β−Sheets, proteins: struct. *Funct. Bioinf.* 2005;61:559–569.

[5] Choe S, Sun XS. Bending elasticity of anti-parallel beta-sheets. *Biophys. J.* 2007;92(4):1204–1214.

[6] Tu ZC, Ou-Yang ZC. Variational problems in elastic theory of biomembranes, smectic-A liquid crystals, and carbon related structures,
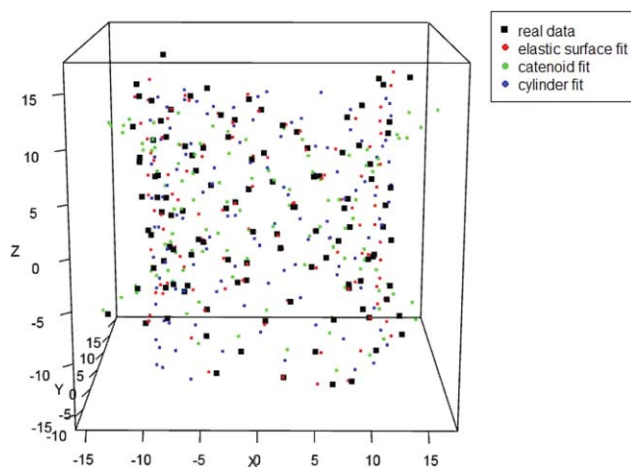

FIGURE 4 LSE for GFP 1myw. Black squares represent real data points. Red, green, and blue dots represent the corresponding fitted elastic surface model, catenoid model, and cylinder model

TABLE 3 LSE results for 1cka by using 3 models

	Catenoid			Cylinder		Elastic surface		
	a	diam./ht.	RMSE	diam./ht.	RMSE	epsilon	diam./ht.	RMSE
1cka	1.15	1.613	0.877	1.22	1.096	0.65	1.16	1.045

In: Seventh International Conference on Geometry, Integrability and Quatization; 2005:237–248.

[7] Toda M, Athukorallage B. Geometry of biological membranes and Willmore energy, In: AIP Conference Proceedings vol. 1558; 2013: 883–886.

[8] Deckelnick K, Grunau HC. A Navier boundary value problem for Willmore surfaces of revolution. *Analysis.* 2009;29:229–258.

[9] Dall'acqua A, Deckelnick K, Grunau HC. Classical Solutions to the Dirichlet Problem for Willmore Surfaces of Revolution. *Adv Calc Var.* 2008;1:379–397.

[10] Helfrich W. Elastic properties of lipid bilayers: theory and possible experiments. *Z. Naturforsch.* 1973;28(11):693–703.

[11] Pulov V, Hadzhilazova M, Mladenov I. Symmetries and some special solutions of the Helfrich model. In: Ganghoffer JF, Mladenov I, eds. *Similarity and Symmetry Methods*. Springer International Publishing; 2014:353–364.

[12] Vassilev V, Mladenov I. Conservation laws and group-invariant solutions of the Willmore equation. In: Mladenov I, Hirshfeld A, eds. *Geometric Symmetry Groups*. SOFTEX, Sofia; 2004:246–265.

[13] Vassilev V, Djondjorov P, Mladenov I. Lie group analysis of the Willmore and membrane shape Equations. In: Ganghoffer JF, Mladenov I, eds. *Similarity and Symmetry Methods*. Springer International Publishing; 2014:365–376.

[14] Willmore T. *Riemannian Geometry*. Oxford: Clarendon Press; 1996.